Published on the web June 12, 2010

Novel Method for Construction of a Metal–Organic Monolayer–Si Structure Utilizing Thiol-terminated Monolayer Covalently Bonded to the Surface through Si–C Bonds

Hitoshi Fukumitsu,[1,2] Takuya Masuda,[1,2] Deyu Qu,[1] Yusuke Waki,[1] Hidenori Noguchi,[1,2,3] Katsuaki Shimazu,[4] and Kohei Uosaki*[1,2,3]

[1]*Division of Chemistry, Graduate School of Science, Hokkaido University, Sapporo, Hokkaido 060-0810*
[2]*Innovative Center of Nanomaterials Science for Environment and Energy (ICNSEE), National Institute for Materials Science (NIMS), Tsukuba, Ibaraki 305-0044*
[3]*International Center for Materials Nanoarchitectonics (MANA), National Institute for Materials Science (NIMS), Tsukuba, Ibaraki 305-0044*
[4]*Group of Functional Chemistry, Section of Environmental Materials Science, Faculty of Environmental Earth Science, Hokkaido University, Sapporo, Hokkaido 060-0810*

(Received May 17, 2010; CL-100475; E-mail: UOSAKI.Kohei@nims.go.jp)

An organic monolayer with a thiol group at its end was formed on a hydrogen-terminated (H–) Si(111) surface via Si–C covalent bond by hydrosilylation. $PtCl_4^{2-}$ complex ions were then immobilized on the thiol-terminated monolayer by immersing the substrate in an aqueous solution of K_2PtCl_4 using a strong interaction between the Pt complex and thiol groups. The immobilized Pt complexes were then reduced to Pt nanocluster by $NaBH_4$. Precise surface structure was characterized and it is proven that Pt species were indeed deposited only on top of the thiol-terminated monolayer.

Metal layer formation only on top of the organic monolayer (OM) without direct contact between the substrate and the metal layer is essential for the structure to be used in electronic devices.[1–3] Although many attempts have been made to deposit metal on OM to construct metal–OM–substrate sandwich structure utilizing both gas[4–6] and liquid[7,8] phase processes, most attempts have resulted in penetration of the metal into the OM and the deposition of metal layer not only on top of the OM but also at the OM/substrate interface mainly because of the existence of defect sites in the OM and the lack of control of the deposition rate and amount of the deposited metal.

Recently, Kolb and his co-workers reported a new approach to construct a metal–organic monolayer–metal (M–OM–M) sandwich structure,[9] by first immersing the Au(111) substrate modified with self-assembled monolayer (SAM) in an aqueous solution of noble metal complex such as K_2PtCl_4, K_2PdCl_4, and $PhCl_3$, and then reducing the metal complex attached to the SAM in a metal-free solution to form metal clusters. We also reported the construction of M–OM–M structure using dithiol SAM.[10] These results show that strong interactions between terminal groups of SAM and metal, both complexes and reduced metals, as well as the reduction in a metal ion free solution are the key to the successful construction of M–OM–M junctions.

Construction of metal–organic monolayer–semiconductor (M–OM–SC) structure[11] may be more important as far as the development of novel electronics devices is concerned. In particular, silicon is the most attractive semiconductor substrate because novel M–OM–SC devices can easily be incorporated to highly advanced silicon-based electronic technology. Hence, M–OM–SC junctions have been constructed on silicon surfaces modified with OM by using a mercury drop as a top metal electrode.[12] Since a mercury drop cannot be used as a top metal

layer in real devices, it is essential to form an M–OM–SC structure with a top solid metal layer.
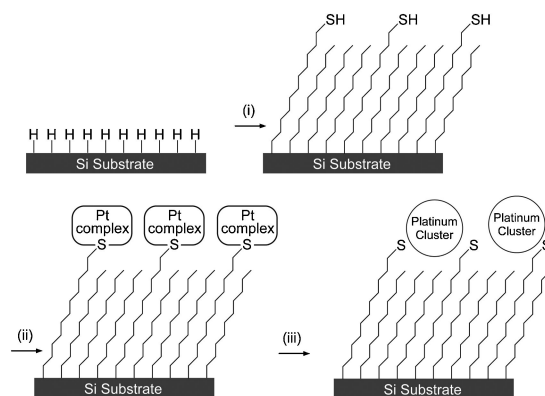
Scheme 1. A schematic illustration of surface modification step.

Here, we propose a novel method for the construction of an M–OM–SC structure with a top platinum layer by following the procedure shown in Scheme 1.

Si(111) wafers (n-type, 1–10 Ω cm) donated by Shin-Etsu Semiconductor were used as a substarate for the formation of H–Si(111) surface by a previously reported procedure.[13–15] The formation of H–Si(111) surface without oxide formation was confirmed by attenuated total reflection Fourier transform infrared spectroscopy (ATR FT-IR) using a parallelogram ATR prism[13,14,25] (Figure 1(a)) and X-ray photoelectron spectroscopy (XPS)[16,25] (Figure 2A(a)).
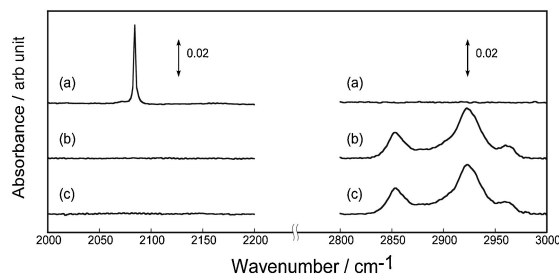
Figure 1. ATR FT-IR spectra of (a) H–, (b) HSC11–, and (c) Pt$_{complex}$–SC11–Si(111) surface.

The H–Si(111) substrate was illuminated with 254 nm light (ca. 3 mW cm^{-2}) for 2 h in a deaerated mixed solution of 1-

decene and 11-mercapto-1-undecene[25] (20:1 by mole fraction) in an Ar-filled glove box (Scheme 1(i)). The mixed solution was used because the formation of a monolayer using neat 11-mercapto-1-undecene was failed with a relatively small monolayer coverage and silicon oxide formation. After this treatment, peaks of C–H stretching vibration were observed in the ATR FT-IR spectrum (Figure 1(b)) and XPS measurement revealed the presence of sulfur[16] (Figure 2B(b)), confirming the formation of monolayer with thiol groups and no oxide formation (Figure 2A(b)). We denote this monolayer-modified Si as HSC11–Si(111), although the majority of the monolayer is of decyl group.
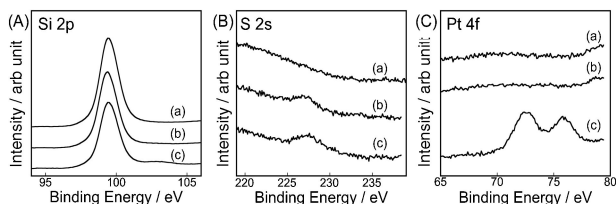
Figure 2. XP spectra in (A) Si 2p, (B) S 2s, and (C) Pt 4f regions of (a) H–, (b) HSC11–, and (c) Pt$_{complex}$–SC11–Si(111) surfaces.

The monolayer-covered substrate was then immersed in a 5 mM aqueous K$_2$PtCl$_4$ solution for 20 min and then rinsed with water (Scheme 1(ii)). The incorporation of Pt(II) complex by this treatment (Pt$_{complex}$–SC11–Si(111)) was confirmed by the presence of Pt bands in XP spectrum[16] (Figures 2C(b) and 3A(a)). The importance of Pt–S chemical interaction for the attachment of Pt complex to the monolayer was proven by the fact that no Pt 4f peak was observed in the XP spectrum of the Pt-treated Si(111) substrate with decyl monolayer, which has no thiol group at its end. The Pt$_{complex}$–SC11–Si(111) substrate was then immersed in a 0.1 M aqueous NaBH$_4$ solution for 1 min to reduce the Pt complex to metallic Pt (Scheme 1(iii): Pt–SC11–Si(111)). XP spectrum of Pt–SC11–Si(111) shows the Pt 4f peak appears at lower binding energy than that of Pt$_{complex}$–SC11–Si(111) (Figure 3A(b)) but still higher than that of bulk Pt,[16] indicating the formation of Pt nanoclusters.[9a] Atomic force microscopy (AFM)[25] also shows the presence of Pt nanoclusters with diameter from a few nm to 10 nm as shown in Figure 3B.
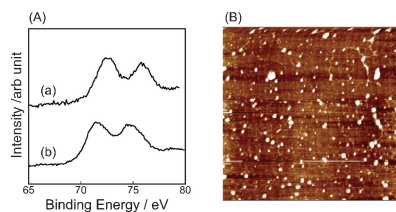
Figure 3. (A) XP spectra in Pt 4f region of (a) Pt$_{complex}$–SC11–Si(111) and (b) Pt–SC11–Si(111) surfaces and (B) AFM image of Pt–SC11–Si(111) surface. 1 μm × 1 μm.

The relative position of each element in the vertical direction was determined by the angle-resolved (AR) XPS measurements.[17] Figure 4 shows the XP spectra of Pt–SC11–Si(111) surface in (a) Si 2p, (b) S 2s, and (c) Pt 4f regions measured at take-off angle, which is defined as the angle between the sample surface and the analyzer axis, of 10, 30, 50,

70, and 90°. As the take-off angle decreased, the intensity of Si 2p peak decreased but those of S 2s and Pt 4f peaks slightly increased, suggesting that the Si(111) substrate was covered with an organic monolayer with thiol groups at its end and that Pt complex was immobilized on top of the molecular layer. Similar results were obtained at Pt$_{complex}$–SC11–Si(111) surface.

More quantitative analysis can be carried out utilizing the relation between the XPS signal intensity from a thin-film-covered substrate and take-off angle, θ, as follows[18]

$$\ln(I) = \frac{-d}{\lambda \sin\theta} + \ln(I_0) \tag{1}$$

where I_0 and I represent the signal intensity at a bare substrate and at a substrate covered with a thin film of thickness d, respectively, and λ is the photoelectron mean free path within the thin film. According to eq 1, $\ln(I)$ should be linearly related to $1/\sin\theta$ with a slope of $(-d/\lambda)$ and an intercept of $\ln(I_0)$. Figure 4(d) shows $\ln$(relative integrated intensity between Si 2p and S 2s peaks) (open circles) and $\ln$(relative integrated intensity between S 2s peak and Pt 4f peak) (closed circles) of the Pt–SC11–Si(111) surface as a function of $1/\sin\theta$. The distance between the thiol group and the Si surface was calculated to be 1.3 nm by using slope for open circles in Figure 4d, $-d/\lambda = -0.38$ and mean free path, λ, for Si 2p photoelectrons in the organic monolayer as 3.4 nm.[19] This thickness is in good agreement with the ellipsometric thickness of the HSC11-monolayer (1.5 nm). Slope for $\ln(I(S)/I(Pt))$ (closed circle in Figure 4(d)) is almost 0, indicating that the position of Pt is the same as that of S, i.e., the outermost part of the monolayer.
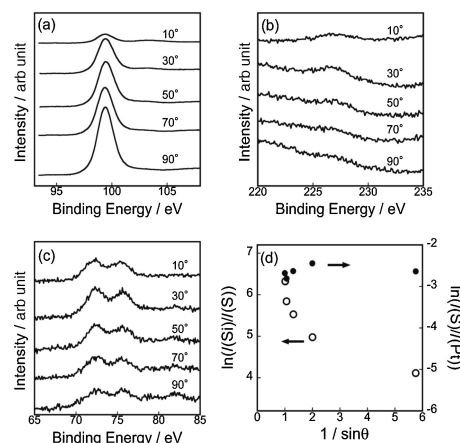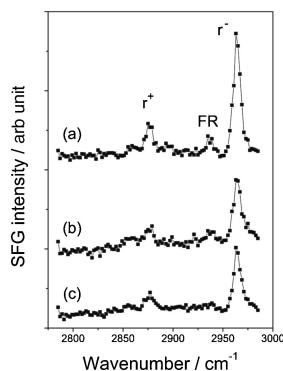

Figure 4. XP spectra of Pt–SC11–Si(111) surface in (a) Si 2p, (b) S 2s, and (c) Pt 4f regions measured at take-off angles of 10, 30, 50, 70, and 90° and (d) $\ln$(relative integrated intensity between Si 2p and S 2s peaks) (open circles) and $\ln$(relative integrated intensity between S 2s and Pt 4f peaks) (closed circles) as a function of $(1/\sin\theta)$.

Several groups have reported that vibrational spectroscopy is quite useful to probe the perturbation of organic monolayer structure caused by the penetration of metal into the monolayer. Richter et al.[20] and Jun and Zhu[21] investigated the structure of octadecyltrichlorosilane (OTS) SAM on SiO$_2$ surface affected by the vapor metal deposition by IR spectroscopy. In both cases, the introduction of conformational disorder in the alkyl chain caused by the penetration of the deposited metal was observed. Bittner et al.[22] carried out sum frequency generation (SFG)

spectroscopy of alkanethiol SAM on Au(111) surface during copper electrodeposition. They showed that even very small amounts of the electrochemically deposited copper can lead to a remarkable change in the CH region of the SFG spectrum due to an interaction between the penetrated metal and the alkyl chain. Recently, we also reported that gauche defects were introduced to alkyl monolayers, which were formed on H–Si(111) surface via Si–C bond as of this study, when metals were deposited by thermal evaporation and sputtering as evidenced by the appearance of methylene bands (d^+ and d^-) in the SFG spectrum, clearly showing the penetration of metal into molecular layer.[6]

Since SFG is quite sensitive to the small change of the conformational order of monolayers, SFG measurements were carried out to prove that Pt did not penetrate into the monolayer and thus Pt is present only on top of the monolayer. The SFG system used in the present study has been described in detail elsewhere.[6,23] Figure 5(a) shows an SFG spectrum in the C–H stretching region of HSC11–Si(111) surface. The three peaks observed at 2876, 2937, and 2963 cm^{-1} can be assigned to the C–H symmetric vibration (r^+), Fermi resonance (FR) between r^+ and C–H bending overtone, and the C–H asymmetric vibration (r^-), respectively, of the terminal methyl (CH$_3$) group of decyl monolayer.[24] No peaks due to the C–H stretching vibration of methylene (CH$_2$) group around 2850 (d^+) and 2920 cm^{-1} (d^-) were observed. This indicates that both decyl and mercaptoundecyl chains in the monolayer are in an all-trans, i.e., highly ordered, conformation.

Figure 5. SFG spectra in the CH stretching vibration region of (a) HSC11–Si(111), (b) Pt$_{complex}$–SC11–Si(111) surface, and (c) Pt–SC11–Si(111) surface.

Figures 5(b) and 5(c) show SFG spectra of Pt$_{complex}$–SC11–Si(111) and Pt–SC11–Si(111) surfaces, respectively. The shapes of the both spectra are similar to that of HSC11–Si(111) surface, although the SFG intensities are smaller than that of HSC11–Si(111) surface (Figure 5(a)). This is in contrast to the results of metal deposition by thermal evaporation and sputtering on the same monolayer.[6] The absence of the C–H stretching vibration bands of methylene shows that no gauche defects were introduced by the incorporation of the Pt complex and its reduction. The ATR FT-IR spectrum also did not change after Pt incorporation (Figure 1(c)). This shows that Pt incorporation does not cause any damage to the highly ordered molecular structure, suggesting that Pt remains only on top of the monolayer. The decrease of the SFG intensity should be due to the attenuation of SFG signal by Pt species on top of the monolayer.

In conclusion, M–OM–SC structure without metal penetration into the monolayer is successfully constructed on a H–Si(111) surface by the following steps. 1. An organic monolayer with a thiol terminal group was formed on a H–Si(111) surface via Si–C bond by UV-induced hydrosilylation. 2. Pt nanoclusters were formed on the monolayer by first immersing the monolayer-covered substrate in an aqueous solution containing PtCl$_4^{2-}$, followed by the reduction of Pt complex in a Pt-free solution. Results of vibrational spectroscopy and ARXPS show the presence of Pt only on top of the monolayer. Further metal deposition to form continuous metal layer by electro- and electroless deposition using Pt as seeds and study of electron-transport properties of the M–OM–Si(111) structure, which are required for the application to electronic devices, are under progress.

References and Notes
1 B. A. Mantooth, P. S. Weiss, *Proc. IEEE* **2003**, *91*, 1785.
2 H. B. Akkerman, B. de Boer, *J. Phys.: Condens. Matter* **2008**, *20*, 013001.
3 R. L. Carroll, C. B. Gorman, *Angew. Chem., Int. Ed.* **2002**, *41*, 4378.
4 T. Ohgi, D. Fujita, W. Deng, Z.-C. Dong, H. Nejoh, *Surf. Sci.* **2001**, *493*, 453, and references cited therein.
5 B. de Boer, M. M. Frank, Y. J. Chabal, W. R. Jiang, E. Garfunkel, Z. Bao, *Langmuir* **2004**, *20*, 1539, and references cited therein.
6 H. Asanuma, H. Noguchi, Y. F. Huang, K. Uosaki, H.-Z. Yu, *J. Phys. Chem. C* **2009**, *113*, 21139.
7 a) M. Nishizawa, T. Sunagawa, H. Yoneyama, *Langmuir* **1997**, *13*, 5215. b) D. Oyamatsu, M. Nishizawa, S. Kuwabata, H. Yoneyama, *Langmuir* **1998**, *14*, 3298.
8 O. Cavalleri, H. Kind, A. M. Bittner, K. Kern, *Langmuir* **1998**, *14*, 7292.
9 a) M. Manolova, V. Ivanova, D. M. Kolb, H.-G. Boyen, P. Ziemann, M. Büttner, A. Romanyuk, P. Oelhafen, *Surf. Sci.* **2005**, *590*, 146. b) F. Eberle, M. Saitner, H.-G. Boyen, J. Kucera, A. Gross, A. Romanyuk, P. Oelhafen, M. D'Olieslaeger, M. Manolova, D. M. Kolb, *Angew. Chem., Int. Ed.* **2009**, *49*, 341, and reference cited therein.
10 a) D. Qu, K. Uosaki, *Chem. Lett.* **2006**, *35*, 258. b) D. Qu, K. Uosaki, *J. Phys. Chem. B* **2006**, *110*, 17570.
11 J. Tanguy, *Thin Solid Films* **1972**, *13*, 33.
12 A. Vilan, O. Yaffe, A. Biller, A. Salomon, A. Kahn, D. Cahen, *Adv. Mater.* **2010**, *22*, 140.
13 G. S. Higashi, Y. J. Chabal, G. W. Trucks, K. Raghavachari, *Appl. Phys. Lett.* **1990**, *56*, 656.
14 S. Ye, T. Ichihara, K. Uosaki, *Appl. Phys. Lett.* **1999**, *75*, 1562.
15 S. Ciampi, J. B. Harper, J. Gooding, *Chem. Soc. Rev.* **2010**, *39*, 2158.
16 C. D. Wagner, W. M. Riggs, L. E. Davis, J. F. Moulder, G. E. Muilenberg, *Handbook of X-ray Photoelectron Spectroscopy*, Perkin-Elmer, Minnesota, **1979**.
17 W. A. Fraser, J. V. Florio, W. N. Delgass, W. D. Robertson, *Surf. Sci.* **1973**, *36*, 661.
18 a) M. Yanagida, T. Kanai, X.-Q. Zhang, T. Kondo, K. Uosaki, *Bull. Chem. Soc. Jpn.* **1998**, *71*, 2555. b) T. Kondo, M. Yanagida, K. Shimazu, K. Uosaki, *Langmuir* **1998**, *14*, 5656.
19 C. D. Bain, G. M. Whitesides, *J. Phys. Chem.* **1989**, *93*, 1670.
20 C. A. Richter, C. A. Hacker, L. J. Richter, O. A. Kirillov, J. S. Suehle, E. M. Vogel, *Solid-State Electron.* **2006**, *50*, 1088.
21 Y. Jun, X.-Y. Zhu, *J. Am. Chem. Soc.* **2004**, *126*, 13224.
22 M. Epple, A. M. Bittner, A. Kuhnke, K. Kern, W.-Q. Zheng, A. Tadjeddine, *Langmuir* **2002**, *18*, 773.
23 S. Nihonyanagi, S. Ye, K. Uosaki, *Electrochim. Acta* **2001**, *46*, 3057.
24 S. Nihonyanagi, D. Miyamoto, S. Idojiri, K. Uosaki, *J. Am. Chem. Soc.* **2004**, *126*, 7034.
25 Supporting Information is available electronically on the CSJ-Journal Web site, http://www.csj.jp/journals/chem-lett/index.html.